Contrastive analysis of trichome distribution, morphology, structure and associated gene expression reveals formation factors in different trichome types of two commercial *Rosa* species.

Wen-Tao Ma[1,2], Min Lu[1], Richard A. Ludlow[3], Dao-Jing Wang[1], Jing-Wen Zeng[1], Hua-Ming An[1,2*]

[1] Guizhou Engineering Research Center for fruit Crops, Agricultural College, Guizhou University, Guiyang 550025, People's Republic of China.

[2] Key Laboratory of Plant Resource Conservation and Germplasm Innovation in Mountainous Region (Ministry of Education), Institute of Agro-bioengineering/ College of Life Science, Guizhou University, Guiyang 550025, People's Republic of China.

[3]School of Biosciences, Cardiff University, Sir Martin Evans Building, Museum Avenue, Cardiff, UK

Hua-Ming An, Corresponding author. Tel: +86-851-88305271 Fax: +86-851-88305271.

E-mail: anhuaming@hotmail.com

Abstract: Trichomes are prevalent on the surfaces of many organs in *Rosa* and have an important impact on the edibility of the fruit. Here, the diversity, distribution, anatomical structure and genetic regulation of trichomes in *Rosa roxburghii* Tratt. (RR) and *R. sterilis* S. D. Shi (RS) are explored. RS and RR are important commercial crops in China due to their nutritional and medicinal values, however their consumption and utilization is limited, in part, by the abundance of trichomes on the fruit. There are two main forms of trichomes in both germplasms, namely glandular and non-glandular trichomes. Non-glandular flagellate and acicular trichomes are observed on the sepals, fruit, major leaf veins and pedicels of both germplasms, but non-glandular branched trichomes are present only on RS. Exfoliation of flagellate trichomes and lignification of acicular trichomes occur gradually on developing fruit. Capitate glandular and bowl-shaped glandular trichomes were abundant in RS, but were only observed on the major leaf veins of RR. Furthermore, some capitate glandular

trichomes on the pedicels were found to develop into prickles in RS. Transmission electron microscopy indicated that vacuolation and in the extraplasmic space occurred in the glandular cells of capitate trichomes at the late secretory stage. Prickles of RR and RS mainly consisted of lignin,suberin,cellulose and hemicellulose, however the ratios of these constituents varied between species. The expression levels of several well-known core trichome regulatory genes varied depending on the trichome types. The transcript abundance of *GL1*, *GL2* and *TTG1* was significantly higher in organs covered with acicular trichomes in both RR and RS, while the highest mRNA level of *TRY* was observed in glabrous organs, suggesting a negative effect of this gene on trichome formation. It was noteworthy that the negative regulatory factor *CPC* was only highly expressed in the leaf mesophyll of RR, where no glandular trichomes were present, but *GL3*, *PDF2-like* and *CPC* transcription factors co-regulated glandular trichome formation in RS. Expression of these genes peaked in the Fb3-stage buds of RR and B3-stage buds of RS, indicating different key phases for the regulation of trichome initiation. These data provide new insights into the genetic control of trichome formation in two *Rosa* species.

Keywords *Rosa*; trichome; morphology; prickle; gene expression

1. Introduction

Trichomes are present on the epidermal surfaces of leaves, stems, sarcocarps, fruits, seeds and other parts of many terrestrial plants (Chen et al., 2014). They originate from epidermal cells and are characterized by their morphology, including whether they are glandular or non-glandular, unicellular or multicellular, branched or non-branched (Werker, 2000). These structures can perform a range of functions for ecological interactions, such as protection against physical or biological stress (Karabourniotis et al., 2020). Furthermore, trichome structure has been used traditionally as an important factor in plant classification (Ma et al., 2016; Sajna et al., 2018).

The mechanisms of trichome initiation and development for unicellular trichomes have been extensively studied in *Arabidopsis* (Hülskamp, 2004; Schellmann and Hülskamp, 2005; Machado et al., 2009). Numerous

studies have identified a set of putative transcriptional regulators (comprising both positive and negative transcription factors) that control the process of epidermal cell development. The positive regulators include R2-R3 type MYB transcription factors GLABRA1 (GL1), the basic helix-loop-helix (bHLH) protein GLABRA3 (GL3) and the WD-repeat protein TRANSPARENT TESTA GLABRA1 (TTG1) (Walker et al., 1999; Zhang et al., 2003). These three positive regulatory proteins together activate trichome differentiation by enhancing the expression of GLABRA2 (GL2) (Serna, 2004). Single-repeat R3 MYB transcription factors CAPRICE (CPC), TRIPTYCHON (TRY), and transcriptional enhancers of TRY and CPC, such as ETC1 ETC2 and ETC3, competitively bind to bHLH factors when they move to the neighboring cells (Gan et al., 2011; Pesch and Hülskamp, 2011; Tominaga-Wada and Wada, 2017). However, unlike unicellular trichomes, relatively little is known about the development and regulatory networks of multicellular trichomes in plants.

Rosa roxburghii Tratt. (RR) is widely distributed in southwest and northwest China, whose fruits are valued for their high levels of ascorbic acid (AsA), superoxide dismutase activity and cancer-preventing effects. *R. sterilis* S. D. Shi (RS) similarly exhibits numerous nutritious and antioxidant activities. RR and RS fruits are being increasingly utilized as functional foods in the food industry to produce preserved foods and desserts, as well as in the beverage industry to produce wine, beer and soft drinks (He et al., 2016; Li et al., 2016). RR and RS belong to the Rosaceae family, and they have a very close genetic relationship based on RAPD and AFLP molecular markers (Wen and Deng, 2003; Wen et al., 2004). However, RR and RS differ in their appearance, the most significant of which are seed abortion and the differences in fruit shape, size and anatomy from RS to RR.

Trichomes are present on the buds, stems, pedicels and fruits of RR and RS, which affect the appearance and perceived quality of the fruits. However, to date, little is known about the formation or regulation of trichomes in these plants. Detailed analysis of trichome types and distribution in vegetative parts of *Rosa* have not been explored in previous studies (Caissard et al., 2006; Asano et al., 2008; Feng et al., 2015). However, He

et al., (1994) and Kellogg et al., (2010) explored the morphological diversity and anatomy in Rosa trichomes. We have also previously reported the types of trichome in two germplasms of *Rosa roxburghii* (Wang et al., 2019). However, the lack of structural studies and exploration of the molecular mechanisms on the development of trichomes have limited the elucidation of molecular pathways. As the current understanding of trichome distribution and development of RR and RS is insufficient, here we analyze the various forms of those structures on stems, sepal., fruit and pedicel in relation to the morphology, distribution, ultrastructure, and histochemistry of the trichomes. Furthermore, changes in relative expression levels of trichome-related genes (*TRY, CPC, GL1, GL2, GL3, TTG1, PDF2* and *PDF2-like*), in both developing buds and *in vitro* organs with different types of trichomes, were studied to provide opportunities for improving the germplasm of *Rosa* through genetic engineering technologies.

2. **Materials and methods**

2.1 Plant material

10-year old trees of *Rosa roxburghii* Tratt. (RR) and *R. sterilis* S. D. Shi (RS) were obtained from the fruit germplasm repository of Guizhou University, Guiyang, China (26°42.408'N, 106°67.353'E). Samples were collected at random and immediately frozen in liquid nitrogen and stored at -80 ℃ until processed.

2.2 Stereo microscopy

The floral bud, stems, leaves, pedicels, sepals and fruits RR and RS were examined using a stereomicroscope (Zeiss Stemi 508) to characterize the types and distribution of trichomes. Samples of floral bud were collected from adult trees (n=30) in early March 2018. The stems, pedicels and sepals were collected from the middle and upper canopy of adult trees (n=30) in middle-late April 2018, and in middle-late August, ripening fruits were obtained from both RR and RS.

2.3 Light microscopy

To investigate the anatomical structure and development of trichomes, the stems, young fruit and floral buds of differing developmental stages of both RR and RS were fixed in formalin, alcohol and acetic acid solution (FAA)(mixture of 50% ethanol, 5% acetic acid, 3.7% formaldehyde, and 41.3% water). Samples were embedded in paraffin wax and longitudinal and transverse sections (6-8 µm thick) of stems and fruits were taken (Johansen, 1940). Sections were stained with 0.05 % toluidine blue (pH 4.3) and 0.5 % fast green, then examined and photographed using a Leica light microscope.

2.4 Scanning Electron Microscopy

The floral buds, young fruits, pedicels, bearing branches, sepals and stems were harvested at various stages of growth from RR and RS and were immediately fixed in 3 % glutaraldehyde solution in 0.1 M phosphate buffer at pH 7.2, overnight at 4 °C. The plant material was dehydrated through a tert-butanol and ethanol mixture series (30, 50, 70, 90, and finally 100 % concentration three times) then dried via vacuum cryodesiccation. Samples were next sputter-coated with gold and viewed using S-3400N scanning electron microscope to examine the type and morphology of trichomes (Ma et al., 2016). The prickles and various trichome types were measured in terms of their total length and basal width from > 20 images per organ.

2.5 Transmission Electron Microscopy

Samples of flagellate, acicular and capitate trichomes, and young prickles, from RR and RS were fixed in 3 % glutaraldehyde for 2 hours and washed thoroughly with 0.1 M phosphate buffer (pH 6.8). Afterwards, they are post-fixed with 1 % osmium tetroxide in phosphate buffer and subjected to following dehydration procedure in alcohol (50, 70, 80,90, and 100 %, each of 10 min), then two changes in 100 % acetone (each of 15 min), and embedded in epoxy resin. Ultrathin sections (80 nm) were transferred to formvar-coated grids and poststained with uranyl acetate and lead citrate (Ma et al., 2016). Observations were made with JEM-1200EX scanning transmission electron microscope at 120KV.

2.6 Flow cytometry analysis

Prickles from RR and RS were isolated and pooled as a sample and cells from the leaves of RR were used as a control. Nuclei from prickles or leaves were prepared and stained with 4',6-diamidino2-phenylindole (DAPI) and a CyFlow Space (Sysmex, USA) analyzer was used to assess the relative DNA content in each sample (Galbraith et al., 2001).

2.7 Fourier transform infrared spectroscopy

Prickles from ripe fruits and stems of RR and RS were gently removed and pooled as a sample in mid August. The dry, milled lignin samples (sample and KBr tableting into a very thin film with a diameter of 13mm) were analyzed with a NICOLET iN10 MX Fourier transform infrared spectrometer, to investigate the IR bands and absorbance patterns of prickle and fruit spines, to assess the functional groups within the lignified cell wall (Li et al., 2012). Background spectra were taken in terms of every sample before getting sample spectra. Each spectrum was scanned 64 times across the range of 4000 to 600 cm^{-1}, with a spectral resolution of 4 cm^{-1}.

2.8 Total RNA extraction and qRT-PCR

Tissue samples were collected at varying stages of flower development: three samples were taken on a weekly basis from buds before shooting (B1-3), seven samples were taken through bud development during shooting every three days and finally samples were collected upon inflorescence (Fb1-7) (Fig. 1). Pericarp was sampled by gently pulling a razor over the young fruit and extracting a tissue sample of no more than 1 mm in thickness. Sarcocarp was sampled in an identical fashion, but here the tissue thickness can be up to 2 mm. Total RNA was extracted using a TRIzol RNA Purification Kit (TaKaRa, China). cDNA synthesis was performed according to the PrimeScript RT reagent Kit with gDNA Eraser protocol (TaKaRa, Kyoto, Japan). To identify genes of interest, sequences were compared between trichome related genes in *Arabidopsis* and a transcriptome

database for RR and RS (unpublished), which was built by our group. Ubiquitin (*UBQ*) was used as reference gene to normalize the expression data. Primers used for qRT-PCR were designed with Primer Premier 6 software (Table 1). Quantitative RT-PCR (qRT-PCR) was performed on an ABI ViiA 7 DX system (Applied Biosystems) using SYBR Premix Ex Taq (TaKaRa). The relative gene expression level was calculated according to the $2^{-\Delta\Delta CT}$ method (Livak et al., 2001). Each experiment was performed in triplicate, and each time the experiment included three biological replicates.

3 Results

3.1 Morphology and structure of trichomes

Trichomes are abundant on the surfaces of both vegetative and reproductive organs of RR and RS, including the floral bud, stem, leaf, sepal., and fruit (Fig. 2). However, there are differences in the types of trichomes present on these organs. Broadly, the trichomes present on the surfaces of RR and RS could be split into two main categories: glandular trichomes and multicellular non-glandular trichomes. In RR, the glandular trichomes were only observed on the abaxial side of leaves (Fig. 2D). The prickles on the stem of RR are opposite and solitary on RS (Fig. 2C, 2I).

Scanning electron microscopy identified non-glandular trichomes including flagellate, acicular and branched forms, of varying size and distribution. Flagellate, multicellular and uniseriate trichomes with the distal end of the terminal cells delicate and greatly elongated (Fig. 3A, 3D, 3I). The flagellate trichomes were abundant on the surfaces of immature sepals and pedicels in RR and RS. The acicular trichomes, non-secretory multicellular trichomes were unbranched (Fig. 3A, 3B, 3E,3H) and exhibited a higher variation in density and size in different organs. The acicular trichomes on immature sepals of RR have a wider base than those of RS (Fig. 3A, 3B).

153 Acicular trichomes were present on the immature pedicel of RR, but not in RS. However, the fruit bearing stem
154 and immature stem surfaces of RR did not have trichomes. Unlike RR, RS had branched trichomes with six
155 arms on its sepals (Fig. 3C). Two types glandular trichomes, capitate (Fig. 3B, 3F, 3G, 3J, 3O, 3P) and
156 bowl-shaped glandular trichomes (Fig. 3Q), cover the epidermis of RS. The capitate glandular trichomes are
157 multicellular, non-vascularized and composed of both epidermis and subjacent layers. They consist of glandular
158 heads with multiple layers of epidermal cells and long stalks. The head of the glandular trichome has a wrinkled
159 surface and the accumulation of a secretion was observed in the apical region of the head (Fig. 3G, 3K, 3P).
160 Stomata were occasionally observed on the upper region of glandular heads (Fig. 3G, 3Q). The capitate
161 glandular trichomes are distributed on the surface of many organs in RS but predominantly present on the sepals,
162 immature pericarp and immature pedicel (Fig. 3B, 3F, 3J), and only small number were found on the immature
163 stems (Fig. 3O). Bowl-shaped glandular trichomes were multicellular, non-vascularized, disc-shaped
164 (patelliform) with a concave surface, and two mastoid structures in the center of the surface (Fig. 3Q). These
165 were only observed on immature stems.

166 The types of trichomes observed and their distribution are provided in Table 2. Statistical analysis showed
167 that the flagellate trichomes of RR and RS were statistically different in the size ($P < 0.05$). The acicular
168 trichomes of RR are larger than RS on pericarp ($P < 0.05$), which were no difference in sepals. The capitate as
169 trichomes of RR on the leaf abaxial were significantly larger than those found on all organs of RS ($P < 0.05$),
170 well as of capitate trichomes head width ($P < 0.05$). The trichomes present on pedicels were characterized
171 by having a larger size than trichomes found on all other organs of RS. It was noted that not only the length of
172 prickles but also the basal width of prickles are larger in RR. Prickles reached a final height of 5.04 ± 0.36 mm
173 and base width of 5.08 ± 0.26 mm in RR and final height of 3.18 ± 0.09 mm and base width of 3.939 ± 0.44 mm
174 in RS ($P < 0.05$).

Acicular trichomes on the fruit of RR first developed in an erect manner, growing outwards, perpendicular to the fruit surface (Fig. 4A) and as they developed, they began to curve downwards, finally becoming sharp, pointed hooks with a broad base (Fig. 4B). Acicular trichomes on fruit of RS are widely spaced and small in size (Fig. 4D-E). Unlike acicular trichomes, capitate glandular trichomes grow both in length and in basal width, and fully mature to prickles (Fig. 4E, 4G). However, not all capitate glandular trichomes develop to prickles and there are still many capitate glandular trichomes on the mature fruit and pedicel (Fig. 4E, 4G). The capitate glandular trichomes of RS have faint yellow heads when young and wine-red when mature.

Longitudinally sliced tissue structure of matured prickles of RR and RS were studied using light microscopy (Fig. 5). Initial observations the prickles of RR and RS indicate that they are multicellular and non-vascularized. The surface of prickles was cornified and epidermal cells had thickened cell walls and enlarged vacuoles and were densely arranged. Prickles of RS consist predominantly of epidermal tissue (Fig. 5F), whereas prickles of RR are composed cells of both epidermal and cortical origin (Fig. 5C). Interestingly, a layer was observed which was comparable to the abscission layer of deciduous leaves in RS, however the prickles of RR did not exhibit this layer.

The ultrastructure of trichomes was explored using transmission electron microscopy (TEM). Acicular trichomes appeared highly vacuolated, with the cytoplasm restricted to a narrow peripheral band around the interior of the cell walls. The cells of acicular trichomes on the sepals of RR had different forms, but all were surrounded by a relatively thick cell wall (Fig. 6A, 6B). The epidermal cells were loosely arranged, and the intercellular spaces were large. The small amount of peripheral cytoplasm and plastids were aggregated in the corners of the cells, surrounding large vacuoles. The acicular trichomes on fruits of RR had a similar cellular morphology (Fig. 6C, 6D), the cell of acicular trichomes on fruits closely arranged and a few Golgi apparatus and mitochondria were found. In mature acicular trichomes of RS sepals (Fig. 6E, 6F), the most striking

197 ultrastructural features are the closely arranged cells, the high density of the cytoplasm, and the large size of the
198 nuclei, which also have prominent nucleoli. Plastids were present too, of varying size and shape, having electron
199 dense stroma and occasional starch grains. Vesicle-like structures of different sizes with an irregular outline
200 were also located in cytoplasm; some of these were translucent whilst others contained an osmiophilic core (Fig.
201 6G, 6H).

202 The flagellate trichomes of RR epidermal cells are long and closely arranged (Fig. 7A). They have thick
203 cell walls with a dense cytoplasm, vacuoles of varying size, large nuclei with prominent nucleoli, extensive
204 rough endoplasmic reticulum, and a zigzag-shaped structure. Various plastids had electron dense stroma and
205 occasional starch grains (Fig. 7B). Compared to the flagellate trichomes of RR, the epidermal cells of RS are
206 elliptic and plastids are ameboid or cup-shaped, many being electron-dense and occasionally containing starch
207 granules. Golgi stacks and rough endoplasmic reticulum occur infrequently (Fig. 7C, 7D).

208 The cells of young prickles in RR consist of densely arranged elliptic cells with a thick cell wall. Within
209 the cells, there are varying degrees of vacuolation and osmiophilic secretory material is localized adjacent to the
210 outer periclinal cell wall (Fig. 8A, 8B). Except the nucleolus, no other organelles were observed. The structure
211 of prickles in RS is broadly like those in RR (Fig. 8C, 8D).

212 Glandular trichomes on RS were selected to further study the structure of the capitate trichomes, whereby
213 ultra-thin sections sepal., fruit, pedicel, and stem were examined (Fig. 9). The capitate trichomes have common
214 and distinguishing features in all four organs. The glandular cells have large vacuoles which occupy the
215 majority of the cellular space, with cytoplasm located only in the peripheral region of the cells and numerous,
216 densely stained droplets of secretory product were observed in the periplasmic space. The glandular
217 cells contain starch granules and have plasmodesmata, although these are not as clearly visible in cells from the
218 sepal (Fig. 9A, 9B). The glandular cells from the sepal are markedly different, containing other organs and the

cells are polygonal in shape and loosely arranged.

The FTIR spectra of prickles from fruit are shown in Fig.10 (A, B). The spectra of RR and RS are largely similar, and the peaks predominantly ranged from 800-1800 cm^{-1}. The main peaks, which are the stretching vibrations of -OH and suberin, are at 3403 and 2918 cm^{-1}. The bands at 1452, 1383, 1250, 1157 and 1105 cm^{-1} are indicative of lignin and cellulose. However, between RR and RS, the relative intensity of peaks are different. The prickles on stems of RR and RS are mainly composed of lignin, suberin, cellulose and hemicellulose, but that the chemical composition of the prickle of stems is different (Fig. 10C, 10D). The FTIR absorbance was notably higher in the prickles from stems of RS than RR. Furthermore, the two species varied in the peak at 1379 cm^{-1}; in RS this peak is intense but in RR it appears as little more than a shoulder.

To determine whether endoreduplication contributed to the enlarged RR and RS trichome cells, we measured the DNA content of mature fruit prickles using flow cytometry. As shown in Fig. 11, both RR and RS displayed a peak of DNA content at around 200. Surprisingly, no difference in nuclear ploidy levels was observed between fruit prickles and leaf tissue (2C), suggesting that RR and RS prickle cells did not undergo any endoreduplication.

3.2 Trichome-related gene expression in organs with different trichome types.

Above we report the distribution and structure of different types of trichomes, homogenous or heterogenous in their distribution over various organs, providing a basis for the exploration of regulatory mechanisms governing trichome formation and differentiation at specific developmental stages. Based upon previous findings about trichome formation factors in other plants, eight trichome-related genes were studied to assess their expression levels in organs with different types of trichomes according to quantitative PCR. Trichome-related genes expression displayed broadly consistent patterns in different trichomes types in some organs of RR and RS (Fig. 12). The expression levels of *GL2, GL3, TTG1* and *PDF2* is known to be

positively related to trichome formation, and here expression was higher in sepal II with acicular trichomes than that in sepal I, which was covered with flagellate trichomes in RR, however, the expression levels of *GL2* and *PDF2-like* was significantly higher in sepal I. Furthermore, the gene which is negatively associated with trichome formation, namely *TRY*, was significantly higher in sepal I, in which no acicular trichomes were observed. Compared to sepal II, which had visible acicular trichomes and glandular trichomes in RS, the expression of *GL1, GL2, TTG1* and *PDF2* was significantly higher in sepal I, and the surface of sepal I was covered with flagellate and branched trichomes. *CPC,* a gene that has been known to function in suppressing trichome initiation was significantly higher expressed in sepal I, compared to sepal II. Comparing the hairless sarcocarp and pericarp, of which both were covered with acicular trichomes in RR, the expression levels of *GL1, GL2* and *TTG1* were higher in the pericarp than the sarcocarp. The *TRY* gene also exhibits opposite trends with the positive regulatory factors. The qPCR data presented here demonstrates that the expression levels of *GL1, GL2, GL3, TTG1* and *PDF2-like* were significantly higher in pericarp with acicular and glandular trichomes than in sarcocarp of RS. In RR, the expression levels of *GL1, GL2,* and *TTG1* were significantly higher in the pedicel, with acicular and flagellate trichomes, than in the smooth bearing branch. In RS, the expression levels of *GL1, GL2, GL3, PDF2* and *PDF2-like* genes were significantly higher in the pedicel with flagellate and glandular trichomes than in smooth bearing branch. Conversely, expression levels of *CPC* and *TRY* were significantly higher in bearing branch than in the pedicel. The expression levels of *GL1, GL2* and *GL3* were significantly higher in main veins, with profuse acicular and glandular trichomes, as compared to the mesophyll layer, which has no trichomes. Moreover, *CPC*, the gene that has been known to play negative roles in trichome formation, was highly expressed in mesophyll and lowly expressed in main veins. Overall, the expression level of *GL1,GL2* and *TTG1* which are positively regulating trichomes formation are higher in covered with acicular trichomes organs in RR, whereas the *TRY* inhibits trichome formation are expressed higher in lack of trichomes

Organs, and *CPC* only high expressed in mesophyll and higher expression level in in main vein or other trichomes organs, which might be associated with the glandular trichomes formation. Our results show that *GL1* and *Gl2* were expressed at higher levels in acicular trichome organs of RS. Moreover, *GL3* and *PDF2-like* were very high expressed and *CPC* showed the lowest expression in densely glandular trichome organs which maybe shows that these genes significant linked the presence/absence and types of trichomes on the surface of RS.

3.3 Expression profiles of trichome-related genes during bud development

Expression of trichome-related genes in RR and RS were investigated during different stages of bud and floral bud development through qPCR (Fig. 13). Trichome-related genes correlated with bud growth and development. In RS, the total expression of *GL1, GL2, GL3, PDF2-like, CPC* and *TRY* follow a very similar trend through bud development, and the expression levels peaked in development stage B3. Although *TTG1* and *PDF2* have the same trend in bud development of RS, they do not peak at this stage. At the beginning of inflorescence, the positive regulatory genes and the negative regulatory genes showed an increasing trend and reached a peak on B3 in RS, while the trend of RR were slightly different. *GL3, TTG1, PDF2, PDF2-like* and *TRY* showed increased expression during bud development of RR, but did not reach a maximum value and begin to decrease again, except with *PDF2.* The relative expression levels of *GL1* and *CPC* gradually decreased in RR during inflorescence. During inflorescence, the mRNA levels of positive regulatory genes *GL3, TTG1, PDF2, PDF2-like* and the negative regulatory gene *CPC* initially increased before decreasing in RS. However, the time required to reach peak was different; *TTG1, PDF2-like* and *CPC* were Fb3 and the rest were Fb4. In RR, trichome-related genes exhibited a similar pattern, in which initially expression increased then a subsequent decrease were observed, and the peak of almost all genes occurred in stage Fb3.

4 Discussion

Trichomes are hair-like structures that commonly present on the surface of branches, roots, leaves and

285 sepals (Chen et al., 2014; Haratym et al., 2015), and indeed some fruits are also thickly covered with trichomes.
286 The surface of fruits of RR and RS are one such example, being densely covered with trichomes as seen in
287 many species of the *Rosa* family. These trichomes have implications for fruit quality, cultivation, and processing
288 (Singh et al.,2020). Here, two morphologically distinct trichome types were observed, namely glandular and
289 non-glandular trichomes, which have been previously reported in the genus *Rosa*. (Wang et al., 2019). The
290 external and internal features of trichome morphology and subcellular features of two main type trichomes and
291 capitate glandular morphotype were analyzed together here for the first time in RR and RS.

292 Non-glandular trichomes of RR and RS were mainly flagellate and acicular trichomes. These are typical
293 types of non-glandular trichomes from other *Rosa* species, including *Rosa. roxburghii* Tratt f. *esetosa* Ku (Wang
294 et al., 2019) and *Rosa hybrida L.* 'Radtko' (Kellogg et al., 2011). Acicular trichomes had a homogeneous
295 distribution across sepals and fruit of RR and RS, being especially prevalent on the surface of RR fruit. Acicular
296 trichomes are longer than other trichomes; their sharp tips can serve as a mechanical barrier and a defense
297 mechanism for the plant (Fahn, 1952). It has been shown in *Withania somnifera* (L.) Dunal
298 (Solanaceae) by Munien et al., (2015) that trichome density is closely related to insect pest resistance. Acicular
299 trichomes of RR contained a multicellular basal pedestal, which serves to support the trichome and to provide a
300 point of attachment that "anchors" the trichome to the epidermal surface (Fig. 3A, 4B, 5A). Our results found a
301 difference in the structure of acicular trichomes in RR and RS (Fig.4B, 4E). Acicular trichomes of RS do not
302 have as large a basal pedestal as RR which may be the reason for shedding easily from the surface of fruit with
303 the maturing (Gallenmüller et al., 2015).

304 Flagellate trichomes are mainly distributed on the surfaces of sepals and pedicels in both species and
305 flagellate trichomes of RS are longer than RR. Flagellate trichomes were more abundant in RR and were only
306 present on immature organs (Fig. 3A, 3I). This phenomenon may be due to the mature organ's establishment of

307 phytochemical defense mechanism, by which point they no longer need the protection of flagellate trichomes
308 (Munien et al.,2015). Plastids were observed in the cells of flagellate trichomes, which likely contributed to the
309 silver-white coloration on the sepal's surface of RR and RS (Fig. 7A, 7D).

310 Compared with RR, RS had more abundant non-glandular trichome types. In addition to acicular and
311 flagellate trichomes, there are branching trichomes which have not been observed in other *Rosa* species.
312 Non-glandular trichomes have been shown to function in defense against insect herbivores including
313 influencing oviposition, protection against UV light and low temperature, and facilitating seed dispersal
314 (Karabourniotis, et al., 2020).

315 Our results showed that the greatest differences between trichomes of RR and RS were found in glandular
316 trichomes. The glandular trichomes of RS were located on the surface of all above ground organs, however, in
317 RR limited numbers of glandular trichomes could only be found on the abaxial side of leaves. This may indicate
318 that some genes regulating glandular trichomes on RS have different regulatory pathways with RR, which is in
319 agreement with the hypothesis suggested by Wen et al., (2004), whereby RS was suggested to originate from a
320 mutant of male-sterile *R. kweichonensis*. RS carries both capitate and bowl-shaped glandular trichomes, but
321 capitate glandular trichomes were most common. Capitate glandular trichomes were predominantly present on
322 the pedicel and fruits, with sparse distribution on the bearing branch. Capitate glandular trichomes were
323 multicellular, non-vascularized, thick stalked and had large head cells which were composed of 16-34
324 thin-walled cells, with a small number of pores visible in the center of the head (Fig. 3G, 3J, 3K). Stomata are
325 frequently observed in the early developmental stages of glandular trichomes, corroborating previous work in
326 *Vitis davidii* which showed that stomata on glandular trichomes form in the period of rapid cell proliferation and
327 elongation of the upper region epidermal cells (Ma et al., 2016). The development of stomata was not observed
328 in RS, however this may be a result of variance in the sampling period. The head of capitate trichomes often

329 secrete sticky mucilage to trap insects which can aviod the invasion of insects (Nogueira et al., 2013; Uzelac et
330 al., 2017). Similarly, capitate glandular trichomes can secrete substances via pore-like openings on each of the
331 multicellular head cells based on our observation (Fig. 3G). The nucleus is surrounded by plastids containing
332 starch grains and plastoglobuli, and the cytoplasm contains osmiophilic droplets, mitochondria and endoplasmic
333 reticulum, all of which, in combination, are considered to be evidence of secretory activity in a range of
334 angiosperm taxa (Haratym et al., 2017). However, we observed the ultrastructure of the head of capitate
335 trichome in RS and did not see evidence for such secretion. It may be the case that these trichomes are only
336 secretory at specific developmental stages.
337 During observation of the pedicel of RS (Fig. 3J, 4F, 5E), we initially only saw capitate glandular and
338 flagellate trichomes from tissues harvested in April. As time progressed, prickles were observed on the surfaces
339 of RS pedicels, however our sampling schedule did not allow us to see the early developmental stages of these
340 prickles. Morphologically, there is no difference between glandular trichomes and prickles, but prickles are
341 more robust (Coyner et al., 2005). We surmise that the prickles undergo early developmental stages like other
342 capitate glandular trichomes (Fig. 3J) and once some capitate glandular trichomes have reached the
343 post-secretory phase (Fig. 3G), the heads are shed and they increase in both height and basal width, thus
344 developing into prickles (Fig.4G). Therefore, it is reasonable to presume that the prickles of RS are homologous
345 to capitate glandular trichomes. Rose and raspberry prickles progress through the four stages: (I) prickle is
346 defined simply as a mass of proliferating cells, (II) a stalk emerges from the epidermis at the base of the cell
347 mass and lifting it distally from the stem, (III) the distal cell mass falls off the stalk, followed by cell expansion
348 in the stalk, (IV) the prickle is lignified and growth halted (Kellogg et al., 2011). This progress is similar with
349 RS. However, it is important to note that only a small subset of glandular trichomes complete this final stage of
350 development and form prickles in RS (Fig. 1F, G, 4E, 4G), this differs from *Vitis. Davidii*, where all form

351 prickles (Ma et al., 2016). The glandular trichome head may send signals to the epidermal and/or cortical organs
352 that cause a proliferation of cells, allowing a prickle to develop (Kellogg, 2011).

353 Prickles lack internal vascular material and result from multiple cellular divisions of the epidermis (Fig. 5C,
354 5F). The dense cytoplasm had begun to degenerate, with reduced numbers of organelles visible and was located
355 only in the peripheral region of the cells (Fig. 8). A layer was observed which resembled an abscission zone at
356 the base of prickles of RS, where they meet the epidermis (Fig. 5F). Both mature and young prickles could be
357 broken off with little force at this layer, suggesting this abscission zone fully forms early on in the prickle's
358 development. The prickles of RR do not have such a zone (Fig. 5C), but it was previously reported in the
359 prickles of *Rosa hybrida* cv. "Laura" and "Queen Elizabeth" (Asano et al., 2008, Li et al., 2012).

360 Analysis by FTIR showed that prickles on the fruit surface and stem of RR and RS
361 consisted mainly of cellulose, hemicellulose, cork and lignin, but there were significant differences in the
362 relative abundance of these compounds. These findings were similar to previous studies on wood (Asano et al.,
363 2008; Le et al., 2017). Li et al., 2012 studied the anatomical structure and chemical composition in prickles of
364 *Rosa hybrida*, and found that differences in chemical composition of prickles maybe related to the strength with
365 which the prickle adheres to the stem. The concentration of cellulose, hemicellulose, cork and lignin in prickles
366 were higher in RS than RR, both on the fruit surface and stem. This difference may be one of the reasons why
367 prickles on RS are more weakly adhered than those on RR when the fruit is ripe.

368 Genetic analysis in *Arabidopsis* has established a regulatory pathway that controls trichome initiation
369 (Hülskamp and Schnittger, 1998; Hülskamp, 2004). The active WD40-bHLH-MYB complex activates trichome
370 differentiation by directly inducing the expression of a homeodomain-leucine zipper (HD-ZIP) IV gene
371 *GLABRA2* (*GL2*) (Schellmann and Hülskamp 2005). Although it is possible that the regulation pathway of
372 unicellular trichomes is different from that of multicellular trichome, many regulatory factors have the same

effect under different regulation pathways. For instance, Over-expression of *CsTRY, PaTRY*, *PaCPC-like1, PaCPC-like2* and *PaCPC-like3* in *Arabidopsis* resulted in glabrous phenotype (Tang et al., 2012; Zhang et al., 2019). *CsGL3, CsGL1 , MICT（Micro-trichome）, TBH(Tiny branched hair),* and *TRIL（Trichome-less）*encode HD-Zip proteins with different subfamilies; genetic and molecular analyses have revealed that these transcription factors are responsible for the differentiation of epidermal cells and the development of multicellular trichomes in cucumber (Liu et al., 2016). Though qRT-PCR analysis of trichome-related genes in different organs which covered with different types trichomes, we found that most of these trichome-related genes showed broadly consistent patterns of expression in RR and RS. This observation may partly explain the different types trichome in different organs. Based on the expression of trichome-related genes in different organs with different types of trichomes in RR and RS, we have proposed that there are differences in the regulation of trichomes between these two germplasms. Our results indicate that *GL1* and *GL2* affect acicular trichome development in RR and RS, and that *TTG1* and *TRY* acts only in RR. The described regulatory changes may cause the abundance of acicular trichomes and glandular trichomes in RS, and the repression of some trichome-related genes. The *PDF2* of *Arabidopsis* has not been shown to be involved in trichome formation but type I trichome formation is controlled by *PDF2* in tomato (Yang et al., 2011). However, the expression of *PDF2-like* was higher in the pedicel and pericarp, which were covered with glandular trichomes; such diverse expression patterns suggest that *PDF2-like* may be regulating glandular trichomes in RS and a different regulatory pathway occurs in RR. *CPC* plays an important role in the regulation of non-glandular and glandular trichomes, as indicated in plant species including tomato, poplar, and London plane (Tominaga-Wada et al., 2013; Zhang et al., 2019). However, here the expression level of *CPC* in tissues without glandular trichomes are significantly higher than those with. This finding suggested that *CPC* mainly regulates the formation of glandular trichomes in RR and RS.

During three stages of bud and seven stages of floral bud development, all these genes responded to the growth stages, thereby potentially eliciting influence on trichome initiation. However, the expression patterns were inconsistent between RR and RS. In this study, we found maximum expression of *GL1, GL3, TTG1, PDF2, CPC* and *TRY* at the Fb3 stage of floral bud development in RR, but all of these genes had the highest expression at the B3 stage of bud development in RS. Since different types of trichomes were present in RR compared to RS, we reasoned that the Fb3 stage is a critical trichome developmental period of RR, whereas the B3 stage is for RS. The transcripts of *GL1* ,*GL2, GL3, PDF2-like* and *CPC* were expressed highest in the B3 stage of bud and floral bud development in RS, which may be due to the range of developmental stages of buds, and how the glandular and acicular trichomes were clustered on newly growing shoots and leaves. We observed that most trichome related genes have only one peak in Fb3 of floral bud development of RR, whereas the *GL1, GL2* and *TRY* had three peaks in Fb1, Fb3 and Fb5. This may suggest that these genes play vital roles in acicular trichome development and formation in floral buds of RR. These trichome-related genes are highly expressed in young leaf primordia and then progressively decrease as trichomes begin to initiate (Kirik et al., 2005). However, here the expression of these genes peaked at different developmental stages in different organs and correlated with the formation of different types of trichome, suggesting not only a role in trichome initiation, but also formation.

The types, distribution and micromorphology of trichomes in RR and RS were studied and putative regulatory genes identified. The data presented here provides a basis for creating new *Rosa* varieties with desired trichome growth and density through breeding and genetic engineering and helps to understand the complex network of regulatory interactions controlling the development of multicellular trichomes. This is the first report of quantitative analysis of trichome-related gene expression during bud development across different

trichomes types and organs. Future work should focus on validating a set of reference genes related to trichome initiation and growth, and to determine the precise function of these genes in *Rosa*.

Acknowledgements

This work was supported by grants from the Joint Fund of the National Natural Science Foundation of China and the Karst Science Research Center of Guizhou Province (Grant No. U1812401), National Natural Science Foundation of China (31660549) , the Talent Project of Guizhou Province (Project No. 20164016) and the Construction Program of Biology First-class Discipline in Guizhou (GNYL2017009).

References

Asano, G., Kubo, R., Tanimoto, S., 2008. Growth, structure and lignin localization in rose prickle. *Bulletin of the Faculty of Agriculture*. 93, 117-125.

Caissard, J.C., Ronique, B., Magali, M., Lanie, M., Baudino, S., 2006. Chemical and Histochemical Analysis of 'Quatre Saisons Blanc Mousseux', a Moss Rose of the *Rosa damascena* group. *Annals of Botany*. 97, 231-238.

Chen, C.H., Liu, M.L., Jiang, L., Liu, X.F., Zhao, J.Y., Yan, S.S., Yang, S., Ren, H.Z., Liu, R.Y., Zhang, L., 2014. Transcriptome profiling reveals roles of meristem regulators and polarity genes during fruit trichome development in cucumber (*Cucumis sativus* L.). *Journal of Experimental Botany*. 65, 4943-4958.

Coyner, M.A., Skirvin, R.M., Norton, M.A., Otterbacher, A.G., 2005.Thornlessness in blackberries: a review. *Small Fruits Review*. 4, 83-106.

Fahn, A., 1952. On the structure of floral nectarines**.** *Botanical Gazette*. 113, 464-470.

Feng, L.G., Luan, X.F., Wang, J., Xia, W., Wang, M., Sheng, L.X., 2015. Cloning and expression analysis of transcription factor rrttg1 related to prickle development in rose (*Rosa rugosa*). *Arch. Biol. Sci*. 67, 1219–1225.

Galbraith, D.W., Lambert, G.M., Macas, J., Dolezel, J., 2001. Analysis of nuclear DNA content and ploidy in higher plants. *Curr. Protoc. Cytom.* Chapter 7, Unit 7.6.

438 Gan, L.J., Xia, K., Chen, J.G., Wang, S.C., 2011. Functional characterization of *TRICHOMELESS2*, a new single-repeat R3 MYB
439 transcription factor in the regulation of trichome patterning in *Arabidopsis*. *BMC Plant Biol*. 11, 176.
440 Gao, S.H., Gao, Y.N., Cheng, X., Gang, Y., Chang, J., Yang, Q.H, Yang, C.X., Ye, Z.B., 2017. The tomato B-type cyclin gene, *SlCycB2*,
441 plays key roles in reproductive organ development, trichome initiation, terpenoids biosynthesis and *Prodenia litura* defense. *Plant Science*.
442 262, 103-114.
443 Glover, B., Bunnewell, S., Martin, C., 2004. Convergent evolution within the genus *Solanum*: the specialised anthercone develops through
444 alternative pathways. *Gene*. 331, 1-7.
445 Gallenmüller, F., Feus, A., Fiedler, K., Speck, T., 2015. Rose Prickles and Asparagus Spines – Different Hook Structures as Attachment
446 Devices in Climbing Plants. *PLoS ONE*. 10, 1-20.
447 Haratym, W., Weryszko-Chmielewska, E., 2017. Ultrastructural and histochemical analysis of glandular trichomes of *Marrubium vulgare*
448 L. (Lamiaceae). *Flora* 231,11-20.
449 He, J.Y., Zhang, Y.H., Ma, N., Zhang, X.L., Liu, M.H., Fu, W.M., 2016. Comparative analysis of multiple ingredients in *Rosa roxburghii*
450 and *R. sterilis* fruits and their antioxidant activities. *Journal of Functional Foods*. 27, 29-41.
451 He, Y.H., Cao, Y.L., Li, Z.L., Pi, L.D., 1994. The main economic traits and important vitamin content of 22 species of wild rose in China. *J.*
452 *Hort. Sci*. 2, 158–164.
453 Hülskamp, M., 2004. Plant trichomes: a model for cell differentiation. *Nature Reviews Molecular Cell Biology*. 5, 471-480.
454 Hülskamp, M., Misŕa, S., Jürgens, G., 1994. Genetic dissection of trichome cell development in *Arabidopsis*. *Cell*. 76, 555-566
455 Hülskamp, M., Schnittger. A., 1998. Spatial regulation of trichome formation in *Arabidopsis thaliana*. *Seminars in Cell and*
456 *Developmental Biology*. 9, 213-220.
457 Johansen, D. A., 1940. Plant Microtechnique. New York, NY: McGraw Book Co.
458 Karabourniotis, G., Liakopoulos, G., Nikolopoulos, D., Bresta, P., 2020. Protective and defensive roles of non-glandular trichomes against
459 multiple stresses: structure–function coordination. *J. For. Res*. 31, 1-12.

Kellogg, A., Branaman, T., Jones, N., Little, Z., Swanson, J., 2011. Morphological studies of developing *Rubus* prickles suggest that they are modified glandular trichomes. *Botany*. 89, 217-226.

Kirik, V., Lee,M. M., Wester, K., Herrmann, U., Zheng, Z., Oppenheimer, D., Schiefelbein, J., Hulskamp, M., 2005. Functional diversification of MYB23 and GL1 genes in trichome morphogenesis and initiation. *Development*. 132, 1477-1485.

Le, D.M., Nielsen, A.D., Sørensen, H. R., Meyer, A.S., 2017. Characterisation of Authentic Lignin Biorefinery Samples by Fourier Transform Infrared Spectroscopy and Determination of the Chemical Formula for Lignin. *Bioenerg. Res*. 10, 1025-1035.

Li, H., Liu, F., Xi, L., Gao, B., Yan, S., Wang, L., Ma, N., Zhao, L., Yang, C., 2012. Studies on Anatomical Structure and Chemical Composition in Prickles of *Rosa* hybrid. *Acta Horticulturae Sinica*. 39, 1321-1329.

Li, Q.J., Nan, Y., Qin, J.J., Yang, Y., Hao, X.J., Yang, X.S., 2016. Chemical constituents from medical and edible plants of *Rosa roxburghii*. *China Journal of Chinese Materia Medica*. 41, 451-455.

Liu, X.W., Bartholomew, E., Cai, Y.L., Ren, H.Z., 2016. Trichome-Related Mutants Provide a New Perspective on Multicellular Trichome Initiation and Development in Cucumber (*Cucumis sativus* L). *Frontiers in Plant Science.* 7, 1187.

Livak, K.J., Schmittgen, T.D., 2001. Analysis of relative gene expression data using real-time quantitative PCR and the $2^{-\Delta\Delta CT}$ method. *Methods*. 25, 402-408.

Ma, Z., Wen, J., Stefanie, M., Chen, L., Liu, X., 2016. Morphology, Structure, and Ontogeny of Trichomes of the Grape Genus (*Vitis,* Vitaceae). *Frontiers in Plant Science*. 7, 704.

Machado, A., Wu, Y.R., Yang, Y.M., Llewellyn, D.J., Dennis, E.S., 2009. The MYB transcription factor GhMYB25 regulates early fibre and trichome development. *The Plant Journal*. 59, 52-62.

Munien, P., Naidoo, Y., Naidoo, G., 2015. Micromorphology, histochemistry and ultrastructure of the foliar trichomes of *Withania somnifera* (L.) Dunal (Solanaceae). *Planta*. 242, 1101-1122.

Nogueira, A., Ottra, J.H.L., Guimara˜es, E., Machado, S.R., Lohmann, Lu´cia G., 2013. Trichome structure and evolution in Neotropical *Lianas*. *Annals of Botany*. 112, 1331-1350.

Payne, T., Clement, J., Arnold, D., Lloyd, A., 1999. Heterologous myb genes distinct from *GL1* enhance trichome production when overexpressed in *Nicotiana tabacum*. *Development*. 126, 671-682.

Pesch, M., Hülskamp, M., 2011. Role of *TRIPTYCHON* in trichome patterning in *Arabidopsis*. *BMC Plant Biol*. 11, 130.

Sajna, M.., Sunojkumar, P., 2018. Trichome micromorphology and its systematic significance in Asian *Leucas* (Lamiaceae). *Flora*. 242, 70-78.

Schellmann, S., Hülskamp, M., 2005. Epidermal differentiation: trichomes in Arabidopsis as a model system. *International Journal of Developmental Biology*. 49, 579-584.

Singh, K., Sharma, Y.P., Gairola, S., 2020. Morphological characterization of wild *Rosa* L. germplasm from the Western Himalaya, India. *Euphytica*. 216, 41.

Serna, L., 2004. A network of interacting factors triggering different cell fates. *Plant Cell.* 16, 2258-2263.

Tominaga-Wada, R., Nukumizu, Y., Sato, S., Wada, T., 2013. Control of Plant Trichome and Root-Hair Development by a Tomato (*Solanum lycopersicum*) R3 MYB Transcription Factor. *PLoS ONE*. 8, 1-12.

Tan, Z.,.Guo, F.,Yang, F.Q.,Liu, L.Y., Zhang, X.L., Ren H.Z., 2012. Overexpression of Cucumber *CsTRY* Greatly Represses Trichome Formation in *Arabidopsis. Acta Horticulturae Sinica.* 39, 91-100.

Tominaga-Wada, R., Wada, T., 2017. Extended C termini of *CPC*-LIKE MYB proteins confer functional diversity in *Arabidopsis* epidermal cell differentiation. *Development*. 144, 2375-2380.

Uzelac, B., Janoevi, D., Stojii,D., Budimir, S., 2017. Morphogenesis and developmental ultrastructure of *Nicotiana tabacum* short glandular trichomes. *Micosocopy Research and Technique*. 80, 779-786.

Walker, A.R., Davison, P.A., Bolognesi-Winfifield, A.C., James, C.M., Srinivasan, N., Blundell, T.L., Esch, J.J., Marks, M.D., Gray, J.C., 1999. The TRANSPARENT TESTA GLABRA1 locus, which regulates trichome differentiation and anthocyanin biosynthesis in *Arabidopsis*, encodes a WD40 repeat protein. *Plant Cell*. 11, 1337-1350.

Wang, D.J., Zeng, J.W., Ma, W.T., Lu, M., An, H.M., 2019. Morphological and Structural Characters of Trichomes on Various Organs of

Rosa roxburghii. Hortscience. 54, 45-51.

Wen, X. P., Deng, X.Y., 2003. Characterization of genotypes and genetic relationship of Cili (*Rosa roxburghii*) and its relatives using RAPD markers. *Journal of Agricultural Biotechnology*. 22, 376-383

Wen, X.P., Pang, X., Deng, X.Y., 2004. Characterization of genetic relationships of *Rosa roxburghii* Tratt. and its relatives using morphological traits, RAPD and AFLP markers. *The Journal of Horticultural Science and Biotechnology*. 79, 189-196.

Werker, E., 2000. Trichome diversity and development. *Advances in Botanical Research*. 31, 1-35.

Yang, C., Li H., Zhang, J., Luo, Z., Gong, P., Zhang, C., Li J., Wang, T., Zhang, Y., Lu, Y., Ye, Z.B., 2011. A regulatory gene induces trichome formation and embryo lethality in tomato. *PNAS* 108, 11836-11841

Zhang, F., Gonzalez, A., Zhao, M., Payne, C.T., Lloyd, A., 2003. A network of redundant bHLH proteins functions in all TTG1-dependent pathways of *Arabidopsis*. *Development*. 130, 4859-4869.

Zhang, Y., Zhang, J., Shao, C., Bao, Z., Liu, G., Bao, M.Z., 2019. Single-repeat R3 MYB transcription factors from *Platanus acerifolia* negatively regulate trichome formation in *Arabidopsis*. *Planta* 249, 861-877.

FIGURES:

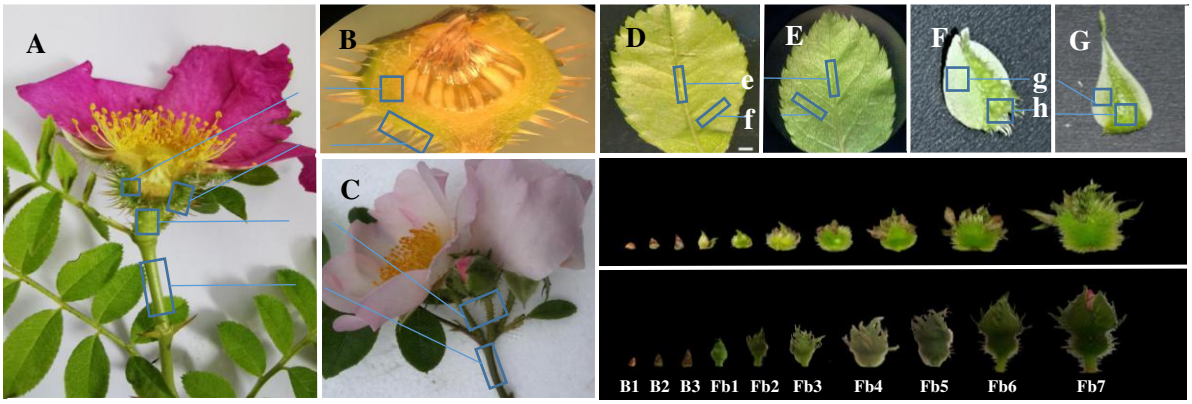

Fig.1 The sampling site of *R. roxburghii* Tratt. (A, D, F, H) and *R. sterilis* S. D. Shi (B, C, E, G, I) for RNA extraction. (a) Sarcocarp; (b) Pericarp; (c) Pedicel; (d) Bearing branch; (e) Vein; (f) Mesophyll; (g) Sepal I; (h) Sepal II.

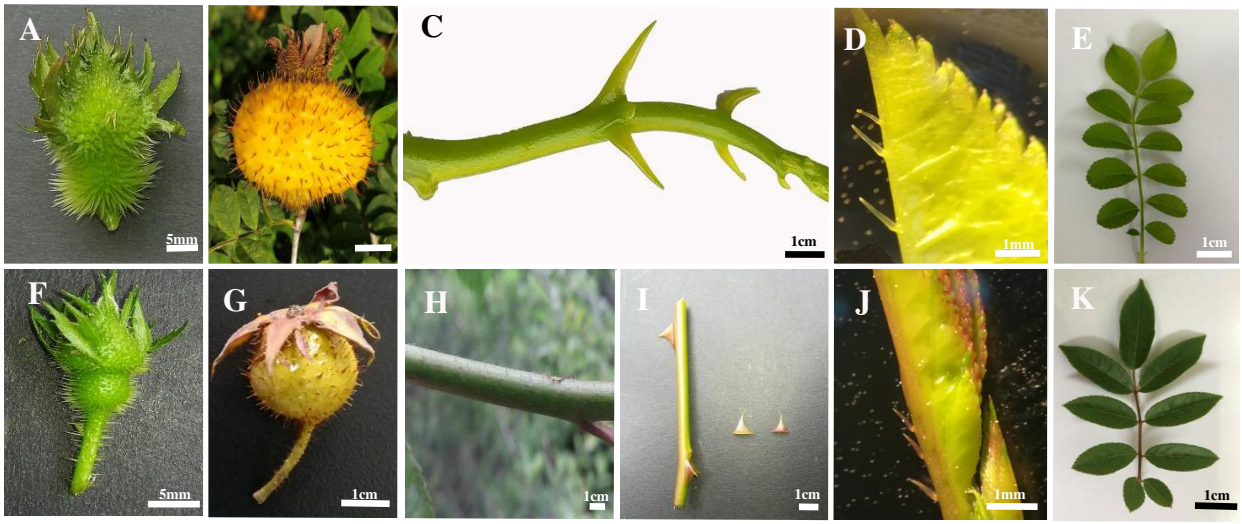

519 **Fig.2.** The macroscopic depiction of *R. roxburghii* Tratt. (A-E) and *R. sterilis* S. D. Shi (F-K) organs. (A) Floral bud; (B) Ripe fruit;
520 (C) Stem; (D) Leaf abaxial; (E) Leaf adaxial; (F) Floral bud; (G) Ripe fruit; (H) Immature stem; (I) Stem; (J) Leaf abaxial; (K) Leaf
521 adaxial.
522
523
524
525
526
527

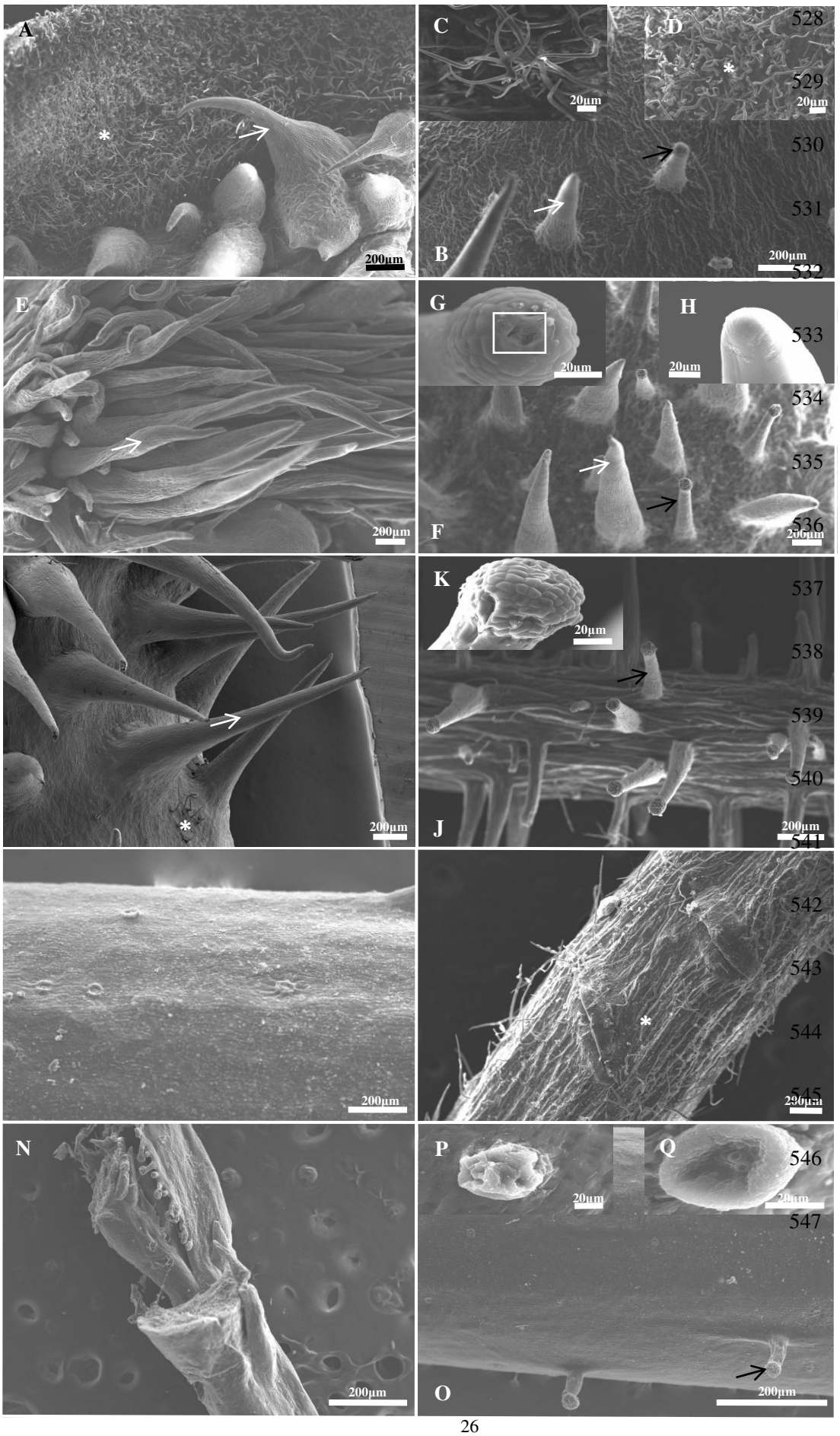
A
200µm
C
20µm
D
20µm
B
200µm
E
200µm
G
20µm
H
20µm
F
200µm
200µm
K
20µm
J
200µm
200µm
200µm
N
200µm
P
20µm
Q
20µm
O
200µm

Fig. 3. SEM of trichomes of *R. roxburghii* Tratt. and *R. sterilis* S. D. Shi (A) flagellate trichomes (stars) and acicular trichomes (white arrows) on immature sepals of *Rosa roxburghii* Tratt.; (B-D): Trichomes on immature sepals of *Rosa sterilis S. D.* Shi. (B) Capitate glandular trichomes (black arrows) and acicular trichomes (white arrows); (C) Branch trichomes; (D) Flagellate trichomes (stars); (E) Acicular trichomes (white arrows) on immature pericarp of RR; (F-H): Trichomes on immature pericarp of RS; (F) Acicular trichomes (white arrows) and capitate glandular trichomes (black arrows); (G) Capitate glandular trichomes with an obvious stoma (drawing districts) on the top of glandular head; (H) Acicular trichomes local magnification map; (I) Trichomes on immature pedicel of RR; (J-K) Trichomes on immature pedicel of RS; (J) Capitate glandular trichomes (black arrows); (K) Capitate glandular trichomes local magnification map; (L) Bearing branch of RR; (M) Bearing branch of RS with flagellate trichomes (stars); (N) Immature stem of RR; (O-Q) Immature stem of RS; (O) Capitate glandular trichomes (black arrows); (P) Capitate glandular trichomes local magnification map; (Q) Bowl-shaped glandular trichomes.

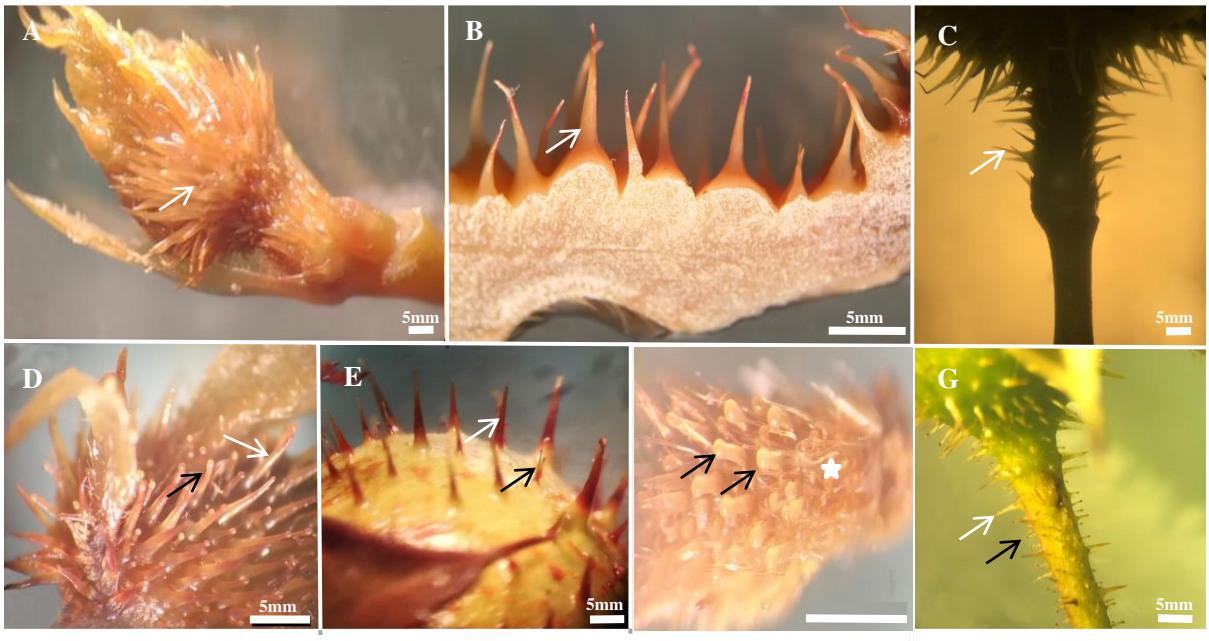

Fig.4. Development of trichomes of *R. roxburghii* Tratt. (A-C) and *R. sterilis* S. D. Shi (D-G). (A) Acicular trichomes (white arrow) on floral bud; (B) Acicular trichomes (white arrow) on fruit; (C) Acicular trichomes (white arrow) on younger pedicel; (D) Capitate glandular trichomes (black arrow) and acicular trichomes (white arrow) on floral bud; (E) Capitate glandular trichomes (black arrow) and acicular trichomes (white arrow) on fruit; (F) Capitate glandular trichomes (black arrow) and flagellate

trichomes (stars) on younger pedicel; (G) Capitate glandular trichomes (black arrow) and acicular trichomes (white arrow) on mature pedicel.

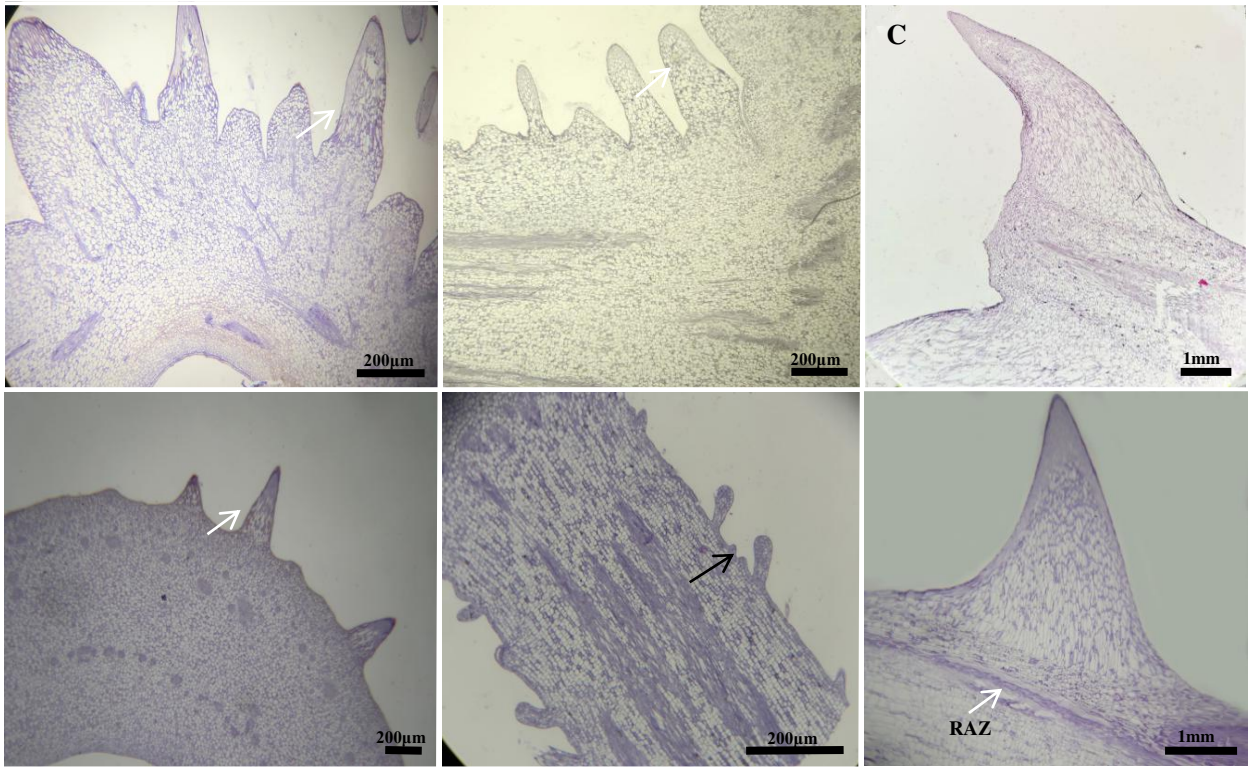

Fig.5. Light microscopy images of acicular trichomes and prickles of *R. roxburghii* Tratt. (A-C) and *R. sterilis* S. D. Shi (D-F) (A) Acicular trichomes (white arrows) on the fruit; (B) Acicular trichomes (white arrows) on the pedicel; (C) Prickle on the stem; (D) Acicular trichomes (white arrows) on the fruit; (E) Capitate glandular trichomes (black arrows) on younger pedicel; (F) Prickle on the stem (RAZ: resembling abscission zone).

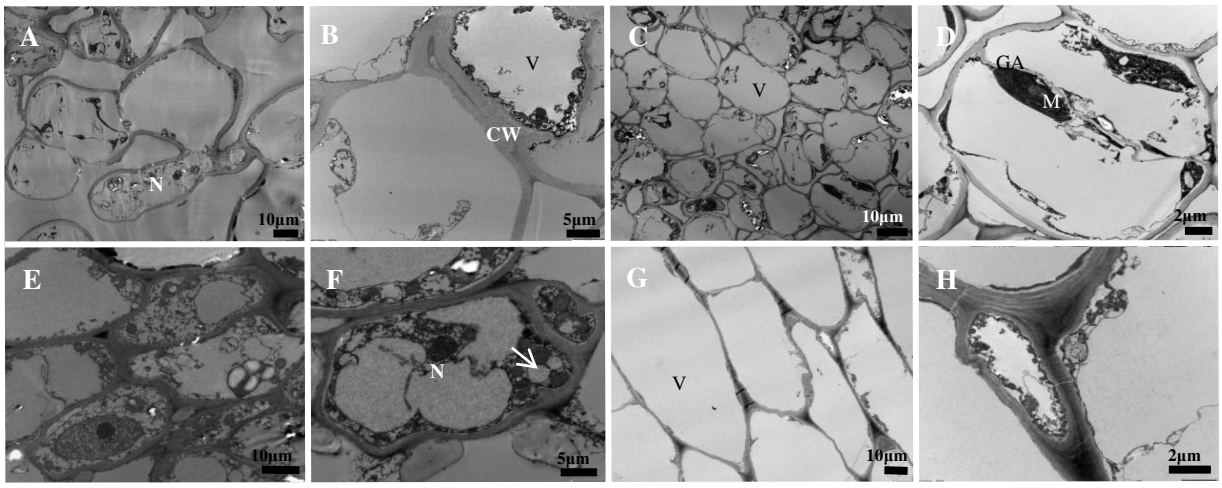

Fig. 6. Transmission electronic microscopic images of acicular trichomes of *R. roxburghii* Tratt. (A-D) and *R. sterilis* S. D. Shi (E-H). (A) Acicular trichomes of sepals; (B) A local magnification map; (C) Acicular trichomes on fruit; (D) C local magnification map; (E) Acicular trichomes of sepals; (F) E local magnification map; (G) Acicular trichomes on fruit; (H) G local magnification map. N: Nucleus; CW: cell wall; V: vacuole; GA: Golgi body; M: Mitochondria.

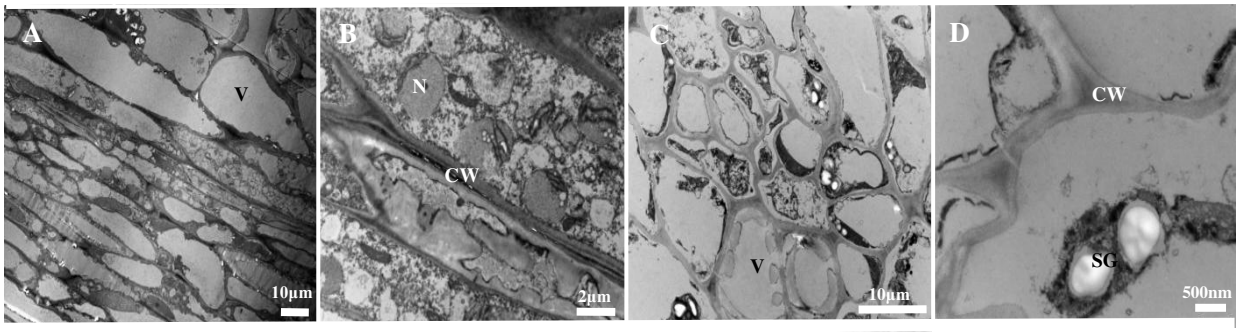

Fig. 7. Sepals with flagellate trichomes of *Rosa roxburghii* Tratt. (A-B) and *Rosa sterilis* S. D. Shi (C-D) viewed by transmission electronic microscopic. Dense thready material (arrow) N: Nucleus; CW: cell wall; V: vacuole; SG:starch grains.

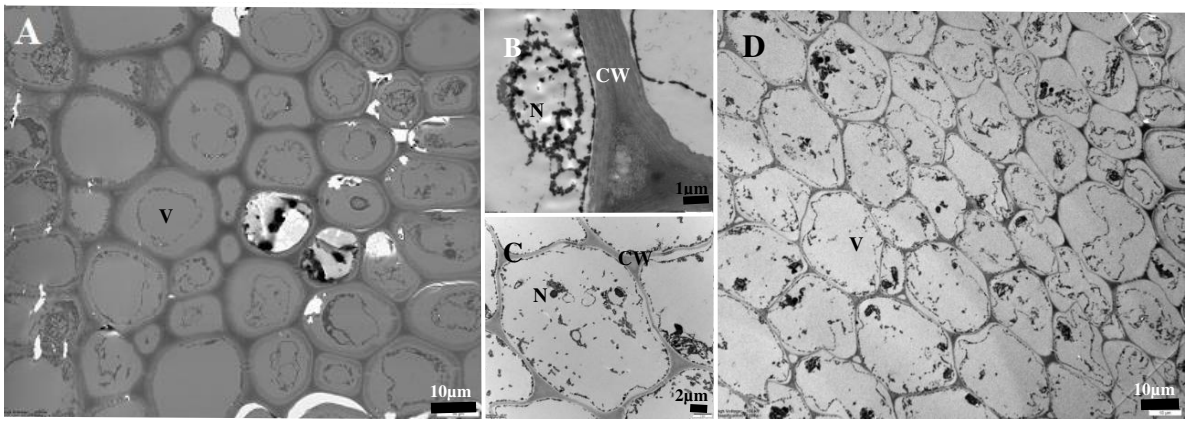

Fig. 8. Transmission electronic microscopic images of young prickles of *Rosa roxburghii* Tratt. (A-B) and *Rosa sterilis* S. D. Shi (C-D). CW: cell wall; V: vacuole.

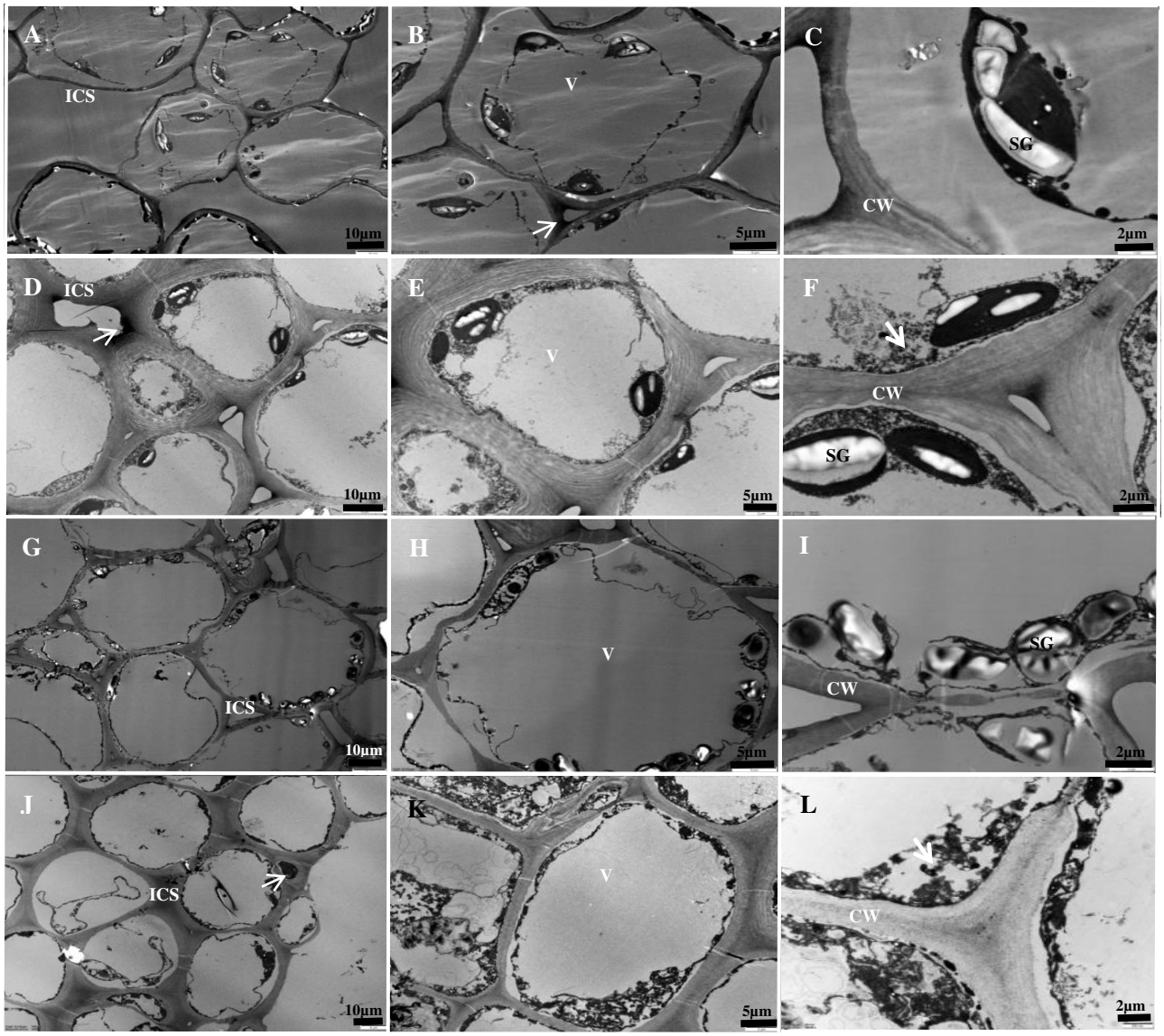

582 **Fig. 9.** Ultrastructure of the head of the capitate glandular trichomes in *Rosa. sterilis* S. D. Shi (A) Capitate glandular trichomes of

583 sepals; (B-C) A local magnification map (arrow indicates stained secretory product); (D) Capitate glandular trichomes of pedicel

584 (arrow indicates stained secretory product); (E-F) D local magnification map (arrow indicate stained secretory product); (G)

585 Capitate glandular trichomes of fruits; (H-I) G local magnification map; (J) Capitate glandular trichomes of stems (arrow indicates

586 stained secretory product); (K-L) J local magnification map (arrow indicates dense granular material) N: Nucleus; CW: cell wall;

587 ICS: intercellular spaces; V: vacuole; SG: starch grains.

588

589

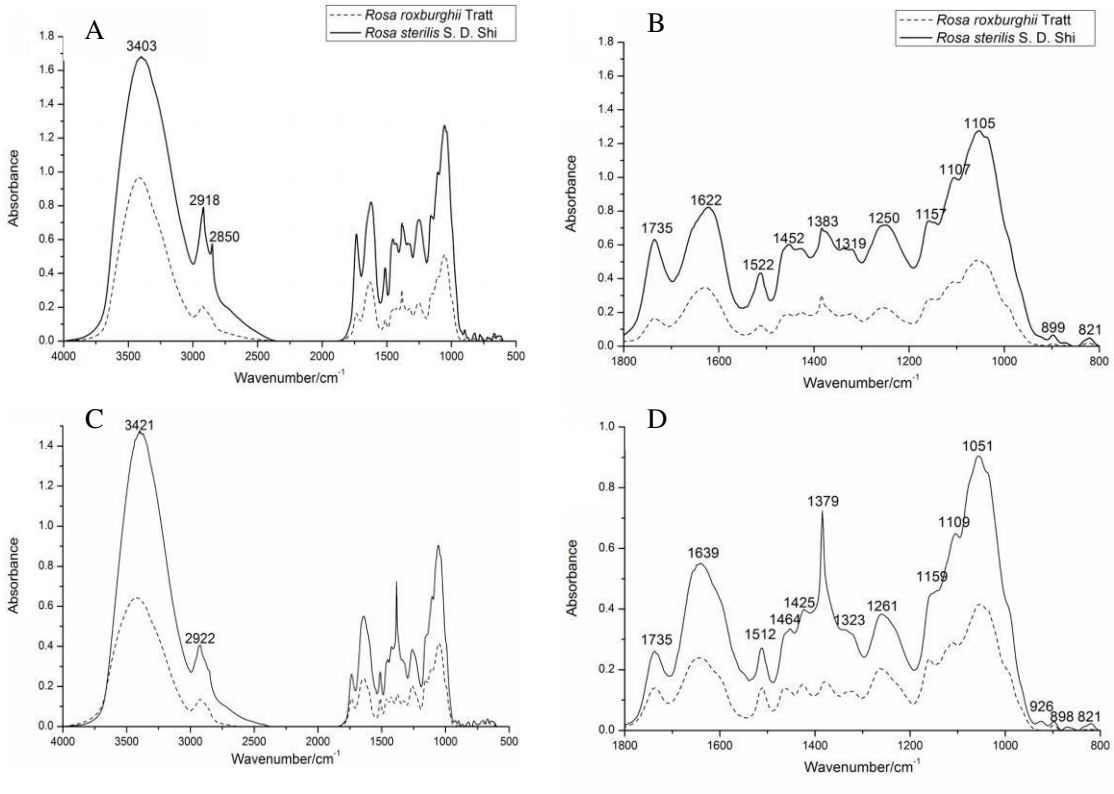

590

591 **Fig.10.** Fourier transform infrared spectra of prickles of fruit and stem in RR and RS. (A) Fourier transform infrared spectra of

592 prickles on fruit in *Rosa roxburghii* Tratt. and *Rosa sterilis* S. D. Shi; (B)A Partial enlargement map; (C) Fourier transform infrared

593 spectra of prickles on stem in RR and RS; (D) C Partial enlargement map.

594

595

596

597

598

599

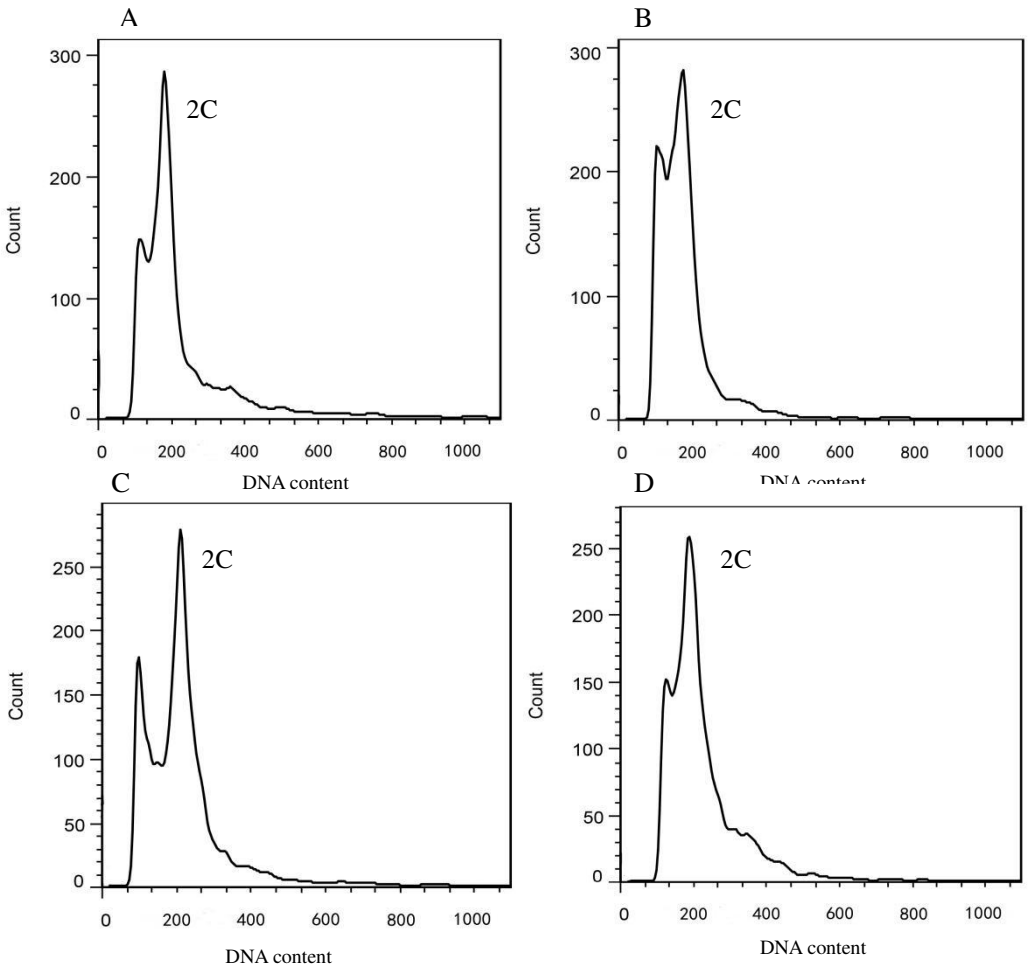

600

601 **Fig.11.** DNA ploidy analysis of *Rosa sterilis* S. D. Shi and *Rosa roxburghii* Tratt. (A) DNA ploidy map of leaves in RS, (B) DNA

602 ploidy map of fruit prickles in RS, (C) DNA ploidy map of leaves in RR, (D) DNA ploidy map of fruit prickles in RR.

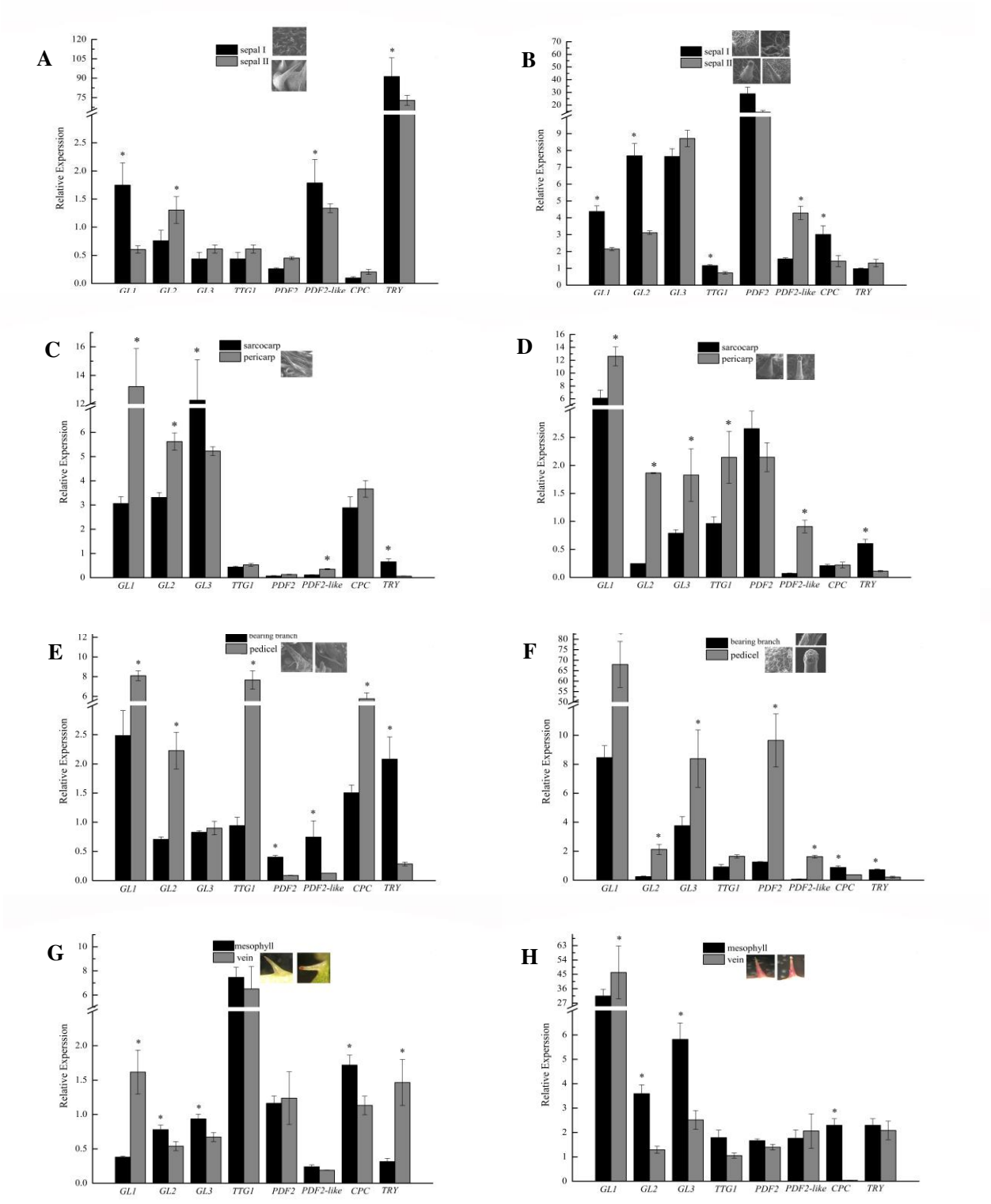

603 **Fig.12.** qRT-PCR analysis of genes related to trichome development in different parts of *R. roxburghii* Tratt. (A, C, E, G) and *R.*

604 *sterilis* S. D. Shiat (B, D, F, H). Values are expressed as the means of at least three independent replicates ± SD. * = significant to p

605 < 0.05.

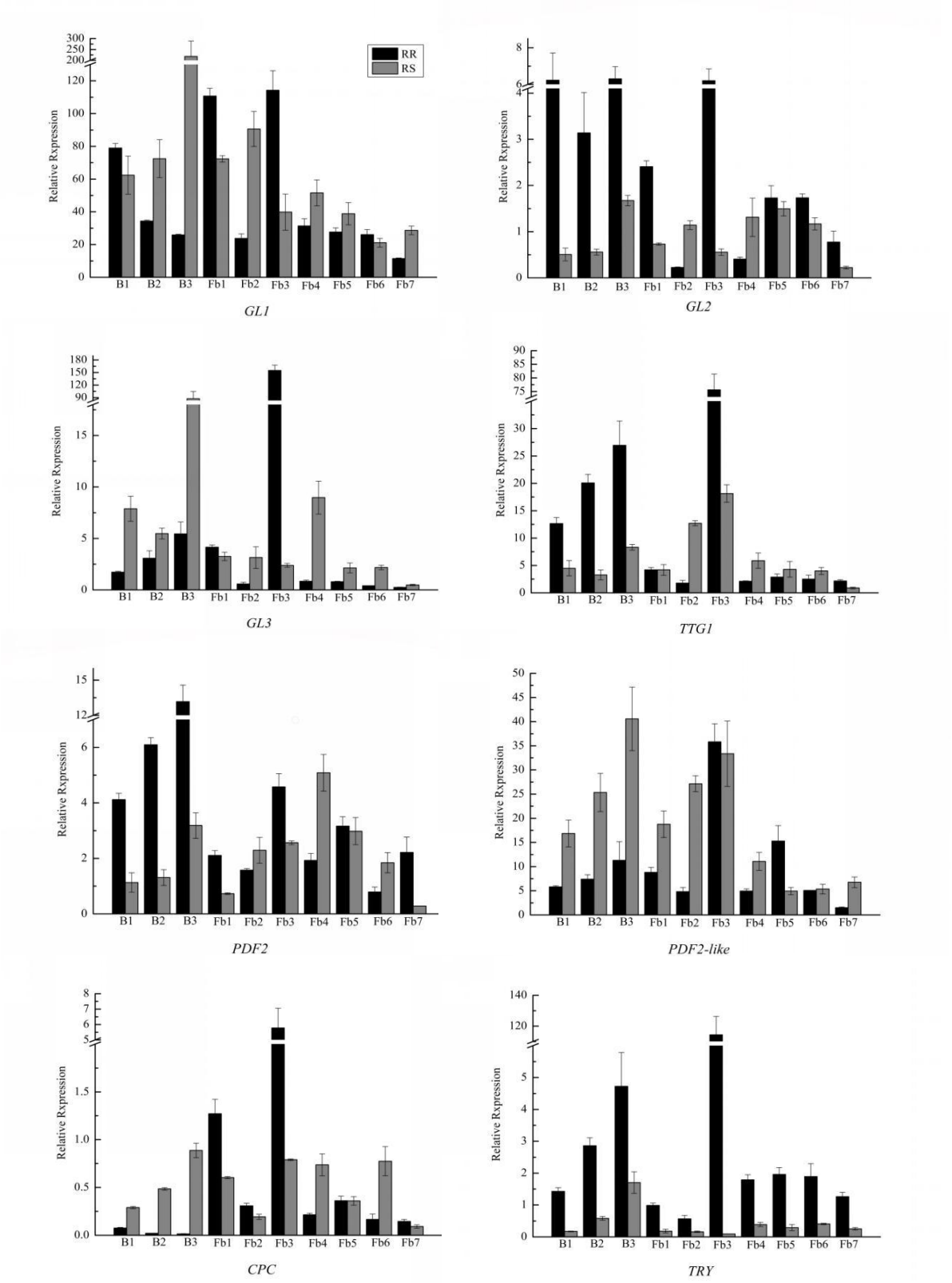

606

607 **Fig.13.** Expression pattern of trichome formation related genes in bud and floral bud of *R. roxburghii* Tratt. and *R. sterilis* S. D. Shi

608 at different development stages. Values are expressed as the means of at least three independent replicates ± SD. Note: B: buds; Fb:

609 flora buds.

610 **Table 1:** qRT-PCR primer information of related genes

Gene name	Primer sequence5'-3'	Gene name	Primer sequence5'-3'
GL1	Forward：GCAGCAGCCACTACCTGATTC Reverse：CCAACACCACTATCTCGACTGATC	*PDF2*	Forward：ACATGCTGCTTACAGTACCTCAC Reverse：AGACTCTGGATGTGCTATCAACTG
GL2	Forward：TAGCAATGGCGAAGGAGACAATAG Reverse：CACCAAGGACGCATCAATGTTATC	*PDF2-like.*	Forward：ATTGACTGTGGATGGAACAACTGG Reverse：TCTCCCCCTCATATCTGAGACCA
GL3	Forward：AGAGCTGGCAGTATATGGATGATG Reverse：TCACCGTTAGGACCGGAGAC	*CPC*	Forward：TTCTTGCTCTAACCGAGACTTGAG Reverse：GGAAGATCAGCAGAGGAGATTGAG
TTG1	Forward：CACGCAATGGCATTCACACTC Reverse：ATGGCGACGATTCTGATGGATAG	*TRY*	Forward：TTAAGGCAGAAGTGAGCAGTATGG Reverse：ACGACTCGGTATGTGTCATTATCC
UBQ	Forward：ATGCAGATYTTTGTGAAGAC Reverse：ACCACCACGRAGACGGAG		

611 **Table 2:** The trichome types, distribution and characteristics (mean ± SE) of *R. roxburghii* Tratt. and *R. sterilis* S. D. Shi Note：

612 "—" showed absent; values are means ± SD (n=30), different small letters in the same column meant significant difference at

613 $P < 0.05$ levels respectively.

Species	Organ	Non-glandular trichome				Glandular trichome	
		Flagellate trichomes (μm)	Acicular trichomes (μm)	Prickle (μm)	Prickle base width (μm)	Capitate glandular trichomes length (μm)	Capitate glandular trichomes head width (μm)
Rosa roxburghii Tratt.(RR)	Sepal	174.03±44.23c	499.82±148.34c	—	—	—	—
	Pericarp	—	1261.99±58.93a	—	—	—	—
	Pedicel	208.51±40.44c	841.27±67.42b	—	—	—	—
	Bearing branch	—	—	—	—	—	—
	Stem	—	—	5047.16±363.27a	5080.24±259.19a	—	—
	Leaf adaxial	—	—	—	—	—	—
	Leaf abaxial	—	443±65.15cd	—	—	833.33 ±134.25a	110±8.47a
Rosa sterilis S. D. Shi (RS)	Sepal	349.79±103.26b	489.53±167.69c	—	—	307.58±122.14c	68.96±6.93b
	Pericarp	—	577.28±149.01c	—	—	324.56±150.22c	70.07±7.02b
	Pedicel	451.28±112.51a	—	—	—	339.56±88.23c	100.63±4.88a
	Bearing branch	221.34±45.21c	—	—	—	—	—
	Stem	—	—	3185.38±95.32b	3934.09±443.68b	185.84±23.64d	88.16±6.34b
	Leaf adaxial	—	—	—	—	—	—
	Leaf abaxial	—	351±26.76d	—	—	603.21±54.15b	76.21±6.87b

614